

Laser Surface Processing of CFRP for Improved Adhesive Bonding

H. K. SEZER^{1,*}, S. VIJAYAKUMAR² AND S. MARIMUTHU³

¹ *Technology Faculty, Gazi University, Ankara, 06500, Turkey*

² *School of Mechanical and Manufacturing, Loughborough University, Loughborough, United Kingdom*

³ *The Manufacturing Technology Centre, Ansty Business Park, Coventry, United Kingdom*

Carbon fibre reinforced polymer (CFRP) composites are increasingly being used in industries from aerospace and automotive to energy (renewable sector especially), medical, sports etc. Adhesive bonding is the preferred method of joining the composite materials, due to its advantages resulting in better in performance; however, the low surface energy of the polymer matrix of the CFRP results in poor adhesion characteristics, which needs to be addressed in order to achieve strong adhesive bonds. This paper investigates ultraviolet (UV) Nd:YAG laser surface treatment of CFRP to achieve surface conditions ideal for adhesive bonding. Contact angle measurement and single lap shear test were used to evaluate the performance of laser processed samples. The experimental results show that a better adhesive bonding performance can be achieved by producing a narrow deep channel over the CFRP surface using laser machining process. Samples processed with a laser fluence of 0.3 and 1.5 J/cm² shows good adhesive bonding and fibre tear failure, compared to the samples processed at low laser fluence.

Keywords: Cleaning, CFRP, laser, resin, surface, UV, processing, manufacturing

1 INTRODUCTION

There has been an exponential increase in demand for lightweight components for enhanced performance and, the realisation of economic and ecological gains. Owing to its unique characteristics, carbon fibre reinforced polymers (CFRPs) are gaining industrial attention [1, 2]. The outstanding

* Corresponding author's e-mail: kursadsezer@gazi.edu.tr

properties of CFRP satisfy market demand across a wide spectrum of industrial applications ranging from the fabrication of aircraft components to prosthetics of artificial limbs in the medical sector [3-5]. This escalating trend in consumption and exploitation of CFRPs is forecasted to continually grow throughout the next decade with an annual growth rate of 16% [6].

Despite the rising demand for CFRPs in many industrial applications, the joining technology of CFRP composite is yet among the primary challenges and concerns in its utilisation [7]. Conventional joining processes, which involve mechanical fasteners [8], can cause stress concentrations while having a negative effect on the lightweight advantage of the component. Of all the joining processes, adhesion bonding is ideal for composites due to a higher degree of flexibility, and more uniform stress distribution with almost no stress concentration locations [9]. Moreover, the adhesion bonding is primarily a laminar substance-to-substance bond, which fundamentally improves [10] the integrity of the final component.

To achieve a strong and resistant adhesive bond, a suitable degree of adhesion must exist between the adhesive and the joining substrates [11]. This is influenced by various factors, including surface wettability, excessive resin layer and residues of mould release agents. Surface wettability of untreated CFRP composites is normally less due to low surface energies causing difficulty [12] with adhesive bonding.

Surface modification is necessary prior to adhesive bonding to deliver a clean, active and slightly rough surface. Various techniques [13, 14] have been used to achieve this surface condition such as grit blasting, chemical treatment, etc. Many of the conventional processes, including grit blasting, chemical treatment are not environmentally sustainable due to the use of dangerous substances, which often require safe handling and environmental disposal after use.

Laser surface modification of CFRP has shown and reported to be a promising technique to clean and provide surface-to-surface cohesion that is both strong and reliable. Burnett [15] investigated the response and effects of surface treatment of indirect composites (i.e. prosthetic composites) with Er:YAG and reported an increased bond strength primarily due to the loss of resin matrix and exposure of filler particles. This result was further supported and endorsed by Belcher [16] through a series of laser scans performed on CFRP composite panels using a frequency tripled Nd:YAG laser (emitting at 1064 nm / 3 \approx 355 nm). Similar results were also obtained by Ozel [17] from surface treatment with Nd:YAG laser at a wavelength of 1064nm, which facilitated an improvement in the bonding strength of CFRP laminates by 39%. Also worth noting is the contribution of Prinsloo [18], who demonstrated a TEA CO₂ laser-based coating removal system for metallic and composite aircraft panels.

The aim of this work is to contribute to the understanding of the effect of ultraviolet nanosecond laser irradiation on the surface characteristics of CFRP composites and subsequently its effect on CFRP adhesive bonding strength. The effects of various process parameters were studied and the key process variables and their effect on the material removal were established.

2 EXPERIMENTAL MATERIALS AND METHODS

The experimental setup was explicitly designed to determine the optimum processing conditions and parameters for creating a surface condition ideal for adhesive bonding of CFRP's. The testing samples were aerospace-grade cross-ply CFRP composite sheets of 3 mm thickness, cut to dimensions of 50×50 mm. The laser source used for this experiments is a Litron frequency tripled Q-switched Nd:YAG laser with a wavelength of 355 nm, maximum pulse frequency of 10 Hz and a pulse duration of 8 ns. The schematic of the experimental setup used to perform the laser surface modification experiment is shown in Figure 1. A square mask was used to achieve a laser beam of uniform spatial intensity from the Nd:YAG laser, which delivers a raw laser beam of 20 mm diameter. Equations (1) and (2) are used for precise control of the lens (150 mm focal length) to mask as well as lens to workpiece distances [19] to achieve the required laser beam size of 0.5mm over the target surface. Samples were held vertically in an X-Y stage and irradiated with a beam normal to the substrate surface.

$$d = \frac{v}{u} \quad (1)$$

$$\frac{1}{f} = \frac{1}{v} + \frac{1}{u} \quad (2)$$

where d is the demagnification, f is the focal length of the lens, u is the mask to lens distance and v is the lens to target distance.

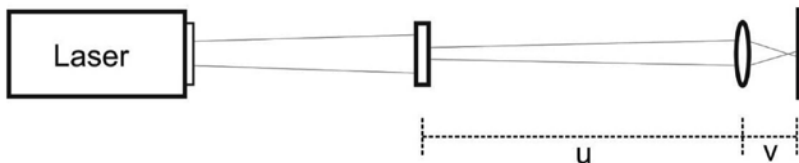


FIGURE 1
A schematic of a typical optical set-up used for CFRP surface machining.

Initial trials were performed with a stationary beam, to estimate the laser ablation characteristics of CFRP and to find the working range of the laser parameters. This was followed by trials over a linear line using a moving beam to find the ablation depth resulting from different laser parameters. By considering the information obtained from spot and linear ablation tests, surface modification was performed over an area by scanning the laser beam with various beam overlaps. All experiments were performed under ambient conditions without the influence of any assisting gas. The laser-treated samples were analysed using optical microscopy, 3D imaging and single lap shear testing. The change in wetting characteristics of the laser processed samples was analysed by measuring the static contact angle [20] by sessile drop technique, by video-based static contact angle computing device.

3 RESULTS AND DISCUSSION

Figure 2 shows the effect of laser energy fluence, pulse frequency and number of pulse (NOP) per position on the ablation depth observed over the CFRP samples. As clearly noticed from the figure, an increase in laser fluence increases the ablation depth, however, laser pulse frequency has no discernible effect on the ablation depth. This may be attributed to the low operating pulse frequency of the Nd:YAG laser (i.e. 2-10 Hz) which essentially means long time delay between the laser pulses (i.e. ~100 ms to ~1 sec). Due to the long pulse off time (or delay i.e. ~100 ms to ~1 sec), the material come back to room temperature and thus pulse frequency has negligible effect on material removal characteristics. The increase in ablation depth with fluence is almost linear.

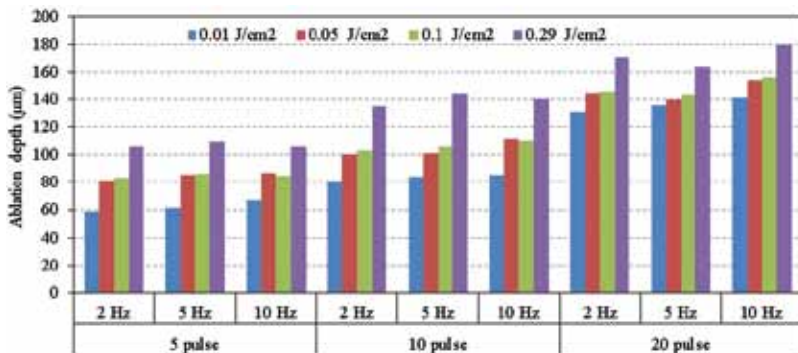


FIGURE 2

Effect of laser energy fluence and laser pulse frequency on CFRP ablation depth.

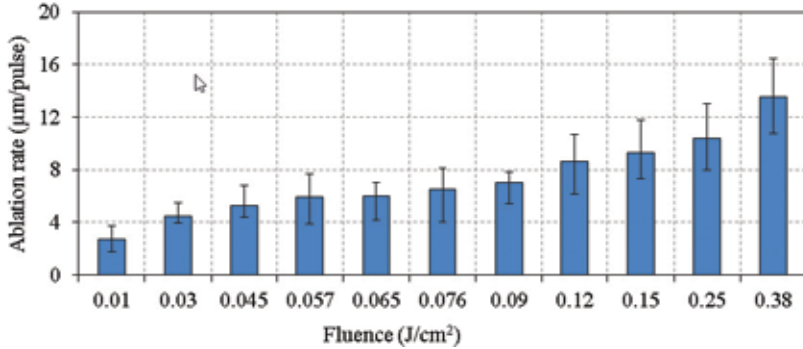


FIGURE 3
Effect of laser fluence on CFRP ablation rate.

Figure 3 shows the effect of laser pulse energy/fluence on the ablation rate (i.e. ablation depth per pulse). As expected, an increase in laser pulse fluence increases the ablation rate per pulse. In addition, as noticed from the figure, the rate of increase in ablation with laser energy fluence is almost linear. This is most likely due to the fact that experimental parametric analysis on the laser energy fluence effect was carried out at operation windows of 0.01 to 0.38 J/cm² which lies above the ablation threshold fluence of the resin, but below the ablation threshold fluence of the carbon fibres.

Table 1 shows the effect of laser energy/fluence and number of pulse on the ablation characteristics of CFRP surface over the range of parameter levels tested. The ideal surface condition, i.e. semi-exposed fibre is marked in green. As clearly observed from the Table, both increasing number of pulse and fluence results in significant removal of resin and exposure of loose fibre (marked in red in Table 1), which has the potential to affect the structural rigidity of the CFRP components. The table also depicts, no exposed (A), semi-exposed (B) and fully exposed (C) fibre scenarios representing the yellow, green and red cells respectively in the Table.

Once the best parameters for stationary laser beam machining of CFRP were identified, line scanning with a moving laser beam was performed. The parameter selection for laser machining of a line using continuous scanning was based on the input parameters and response of the stationary laser beam machining. The scanning speed for a moving laser beam is computed, so as to deliver a similar amount of absorbed energy per unit area. The scanning speed (S) for the moving laser beam is related to the number of pulses in the stationary laser beam (N_s), the pulse frequency of the moving laser beam (v_m) and the length of laser spot size in scanning direction (L_m) by Equation (3):

TABLE 1
Effect of laser parameters on surface conditions observed with spot irradiation.

J/cm ²	0.01	0.03	0.045	0.057	0.065	0.076	0.09	0.12	0.15	0.25	0.38
No. of pulses	1	1	1	1	1	1	1	1	1	1	1
	5	5	5	5	5	5	5	5	5	5	5
	10	10	10	10	10	10	10	10	10	10	10
	15	15	15	15	15	15	15	15	15	15	15
	20	20	20	20	20	20	20	20	20	20	20
	25	25	25	25	25	25	25	25	25	25	25
	30	30	30	30	30	30	30	30	30	30	30
	50	50	50	50	50	50	50	50	50	50	50
	100	100	100	100	100	100	100	100	100	100	100

	spot only partially ablated
	ablation of matrix material
	complete removal of organic material

$$S = \frac{L_m \times v_m}{N_s} \quad (3)$$

The line laser machining was performed for a various number of pulse per position ranging from 5 to 30, with fluence ranging from 0.12 to 0.38 J/cm² and with a constant frequency of 10 Hz, and the results are shown in Table 2. The results obtained with line scanning are in-line with the observations noticed in spot irradiation.

The machining on line scans was then extended to areas by performing a series of overlapping laser beam line scans. The laser beam overlap (%) is calculated using the Equation (4) as:

$$\text{Laser beam overlap (\%)} = \frac{D - x}{D} \times 100 \quad (4)$$

where D is the beam size and x is the ratio of velocity and laser pulse frequency.

Figure 4 shows the effect of the scanning pattern and laser beam overlap on the CFRP surface condition. As noticed from the figure, an increase in beam overlap reduces the machining performance. Zero % overlap produce surface with high peaks and valleys. The number of peaks and their height reduces with increase in beam overlap, resulting in less surface area and surface roughness leading to lower levels of wettability. This is due to the fact

TABLE 2
Effect of laser parameters on surface conditions observed with line irradiation.

Fluence (J/cm ²)	0.12	0.15	0.2	0.25	0.38
NOP per position	25	25	25	25	25
	20	20	20	20	20
	15	15	15	15	15
	10	10	10	10	10
	5	5	5	5	5

	Removal of resin and loose fibre
	Removal of resin without loose fibre

that, free edge material peaks effects are more effectively cleared by increased laser beam overlap.

To further understand the surface characteristic of the laser machined CFRP samples, the wetting envelope was prepared for CFRP samples machined at various laser parameters and the results are shown in Figure 5. The wetting envelope is expected to provide information on the suitability of a surface to bond with an adhesive with known surface tension. The wetting envelope for the laser-treated samples with water and diiodomethane is shown in Figure 5. The graph shows that the total wetting of a commonly used adhesive for the bonding of composite structures can be achieved, and is located within the enclosed area for some laser-treated sample (represented by the circular marker in Figure 5). As noticed from the figure, the wetting envelope is encompassed mostly by the fluence of 0.3 and 1.5 J/cm² and the graph

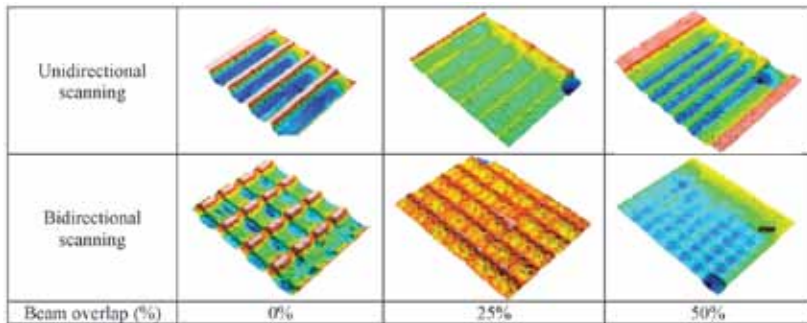


FIGURE 4
Effect of laser beam overlap on CFRP surface condition with unidirectional and bidirectional scanning (fluence = 0.38 J/cm², frequency = 10 Hz, Nop = 5).

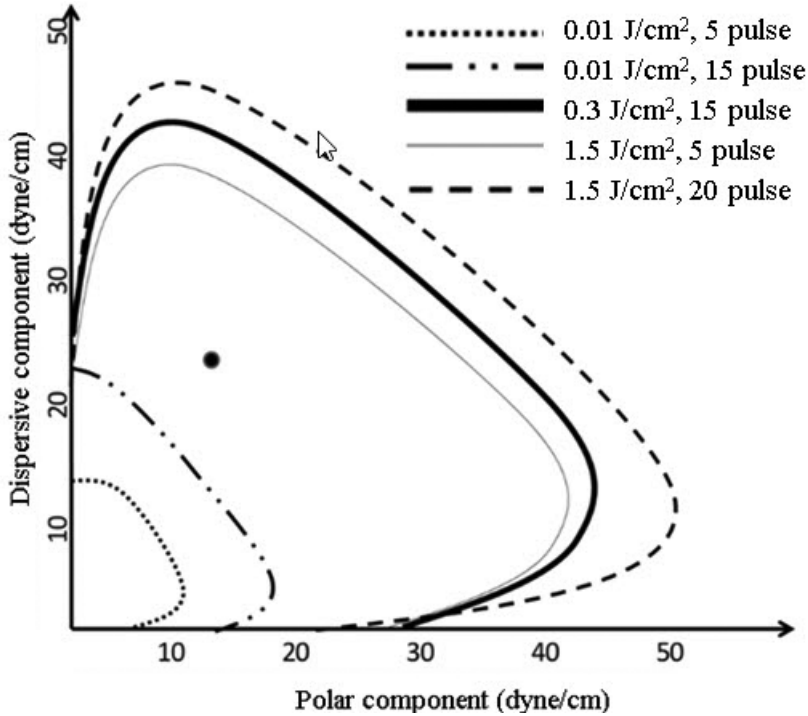


FIGURE 5
Effect of laser parameters on wetting envelope.

predicts that the samples processed at 0.01 J/cm^2 will not be wetted sufficiently by the adhesive.

The effect of laser surface machining on the bonding strength of CFRP-CFRP joints was tested by carrying out a single lap shear test and the results are shown in Table 3. All specimens were prepared with unidirectional scanning at 0% overlap. Five specimens were prepared for each configuration as per the ASTM standard D316. The samples ($25.4 \times 101.6 \text{ mm}$) were bonded together with the adhesive at an overlap of 25.4 mm. The table also shows the observed failure mode for each configuration as cohesive failure (C), adhesive failure (A) and fibre tear failure (FT).

As noticed from Table 3, the shear strength of the sample is closely related to the surface wettability. The samples processed with a laser fluence of 0.3 and 1.5 J/cm^2 shows good adhesive bonding and fibre tear failure (FT), compared to the samples processed at low laser fluence. This should be attributed to better wetting characteristics of the CFRP surface with adhesive as noticed from Figure 5, and a high surface roughness characteristic for zero percentage beam overlap as noticed from Figure 4.

TABLE 3

Failure mode observed for the CFRP bonded samples processed with various laser condition.

Fluence	NOP/ position	Machining depth	Contact angle	Shear strength	Failure mode
J/cm ²		µm	°	MPs	
0.001	5	8	69	7	70% C; 30% FT
0.001	15	32	66	8	70% C; 30% FT
0.3	15	127	<1	13	100% FT
1.5	5	150	<1	13	90% FT; 10% A
1.5	20	273	<1	12	90% FT; 10% A

4 CONCLUSIONS

The laser surface modification of CFRP composite was studied using an Nd:YAG nanosecond laser operating at ultra-violet wavelength. By selecting adequate laser parameters, the surface morphology of the CFRP samples can be tailored to achieve better adhesive bonding strength. Best surface condition for adhesive bonding is achieved with channel-shaped structure over the CFRP, with a high aspect ratio (narrow and deep). A fluence of 0.3 J/cm² results in channel width and depth of 194 µm and 127 µm respectively, which seems to be ideal for adhesive bonding of CFRP. Adhesive bonded CFRP samples with laser-machined channels showed an increase in shear strength by a factor of 4.3 compared to untreated CFRP. Both surface wettability and surface morphology needs to be tailored to achieve the best adhesive bonding strength.

NOMENCLATURE

A	No exposed (A)
A	Adhesive failure (A)
ASTM	American Society for Testing
B	Semi-exposed (B)
C	Fully exposed (C)
C	Cohesive failure (C)
CFRP	Carbon fibre reinforced polymer
cm	Centimetres
CO ₂	Carbon Dioxide
<i>D</i>	Beam size (mm)
<i>d</i>	Demagnification,
Er:YAG	Erbium-doped: yttrium aluminium garnet

f	Focal length (mm)
FT	Fibre tear
Hz	Hertz (frequency)
J	Joules (energy)
L_m	Length of laser spot size in scanning direction (mm)
ms	Micro seconds
Nd:YAG	Neodymium-doped: yttrium aluminium garnet
N_s	Pulses in the stationary laser beam
S	Scanning speed
TEA	Transversely Excited Atmospheric
u	Mask to lens distance (mm)
UV	Ultra-violet
v	Lens to target distance (mm)
v_m	Pulse frequency of the moving laser beam (Hz)
X	Ratio of velocity

REFERENCES

- [1] Sezer H.K. Short Review on Laser Texturing and Cleaning Carbon Fibre Composites for Aerospace Applications. *Journal of Polytechnic* **19**(4) (2016), 623-631.
- [2] Kato M., Kakinuma Y., Shirakawa Y., Iijima K. and Iwashita Y. Positioning Performance Evaluation for Light-Weight Rotary Stage CFRP Application. *International Journal of Automation Technology* **14** (2020), 80-90.
- [3] Quilter, A. 2001, Composites in aerospace applications, IHS White Paper, 444.
- [4] Friedrich K. and Almajid A.A. Manufacturing aspects of advanced polymer composites for automotive applications. *Applied Composite Materials* **20** (2013), 107-128.
- [5] Scholz M.-S., Blanchfield J., Bloom L., Coburn B., Elkington M., Fuller J., Gilbert M., Mufflahi S., Pernice M. and Rae S. The use of composite materials in modern orthopaedic medicine and prosthetic devices. A review, *Composites Science and Technology* **71** (2011), 1791-1803.
- [6] Holmes M. Global carbon fibre market remains on upward trend. *Reinforced Plastics* **58** (2014), 38-45.
- [7] Smith P., Pascoe K., Polak C. and Stroud D. The behaviour of single-lap bolted joints in CFRP laminates. *Composite Structures* **6** (1986), 41-55.
- [8] Giannopoulos I.K., Grafton K., Guo S. and Smith H. Damage tolerance of CFRP airframe bolted joints in bearing, following bolt pull-through failure *Composites Part B: Engineering* (2020), 107766.
- [9] Kim K.-S., Yoo J.-S., Yi Y.-M. and Kim C.-G. Failure mode and strength of uni-directional composite single lap bonded joints with different bonding methods. *Composite structures* **72** (2006), 477-485.
- [10] Encinas N., Oakley B., Belcher M., Blohowiak K., Dillingham R., Abenojar J. and Martínez M. Surface modification of aircraft used composites for adhesive bonding. *International Journal of Adhesion and Adhesives* **50** (2014), 157-163.
- [11] Duncan B., Mera R., Leatherdale D., Taylor M. and Musgrove R. Techniques for characterising the wetting, coating and spreading of adhesives on surface. *Materials Science* (2005), DEPC-MPR 020.
- [12] Wingfield J. Treatment of composite surfaces for adhesive bonding. *International journal of adhesion and adhesives* **13** (1993), 151-156.

- [13] Nattapat M., Marimuthu S., Kamara A. and Esfahani M.N. Laser surface modification of carbon fiber reinforced composites. *Materials and Manufacturing Processes* **30** (2015), 1450-1456.
- [14] Holtmannspötter J., Czarnecki J., Wetzel M., Dolderer D. and Eisenschink C. The use of peel ply as a method to create reproduceable but contaminated surfaces for structural adhesive bonding of carbon fiber reinforced plastics. *The Journal of Adhesion* **89** (2013), 96-110.
- [15] Burnett Jr L.H., Conceição E.N., Pelinos J.E. and Eduardo C.D.P. Comparative study of influence on tensile bond strength of a composite to dentin using Er: YAG laser, air abrasion, or air turbine for preparation of cavities. *Journal of clinical laser medicine & surgery* **19** (2001), 199-202.
- [16] Belcher M.A., Wohl C.J., Hopkins J.W. and Connell J.W. Laser surface preparation for bonding of aerospace composites. *Proceedings of the Institution of Civil Engineers-Engineering and Computational Mechanics* **164** (2011), 133-138.
- [17] Ozel, M. 2002, Behavior of concrete beams reinforced with 3-D fiber reinforced plastic grids. University of Wisconsin--Madison.
- [18] Prinsloo F., Van Heerden S., Ronander E. and Botha L. Efficient TEA CO₂-laser-based coating removal system. in XVI International Symposium on Gas Flow, Chemical Lasers, and High-Power Lasers. *International Society for Optics and Photonics, Proceedings of SPIE* **6346** (2007) 63462Q1- 63462Q-8.
- [19] Marimuthu S., Kamara A., Rajemi M., Whitehead D., Mativenga P. and Li L. Laser Surface Cleaning: Removal of Hard Thin Ceramic Coatings. *Laser Technology: Applications in Adhesion and Related Areas* (2018), 325-377.
- [20] Jagdheesh R., Diaz M., Marimuthu S. and Ocaña J. Hybrid laser and vacuum process for rapid ultrahydrophobic Ti-6Al-4 V surface formation. *Applied Surface Science* **471** (2019), 759-766.